FILE.

INTERNAL DOCUMENT 154.

I.O.S.

Design Parameters and Model Testing for Bencat II

A.R. Packwood

April 1982

Internal Document No. 157

NATURAL ENVIRONMENT RESEARCH COUNCIL

INSTITUTE OF OCEANOGRAPHIC SCIENCES

INSTITUTE OF OCEANOGRAPHIC SCIENCES

Wormley, Godalming,
Surrey GU8 5UB
(042-879-4141)

(Director: Dr. A. S. Laughton)

Bidston Observatory,
Birkenhead,
Merseyside L43 7RA
(051-653-8633)
(Assistant Director: Dr. D. E. Cartwright)

Crossway,
Taunton,
Somerset TA1 2DW
(0823-86211)
(Assistant Director: M. J. Tucker)

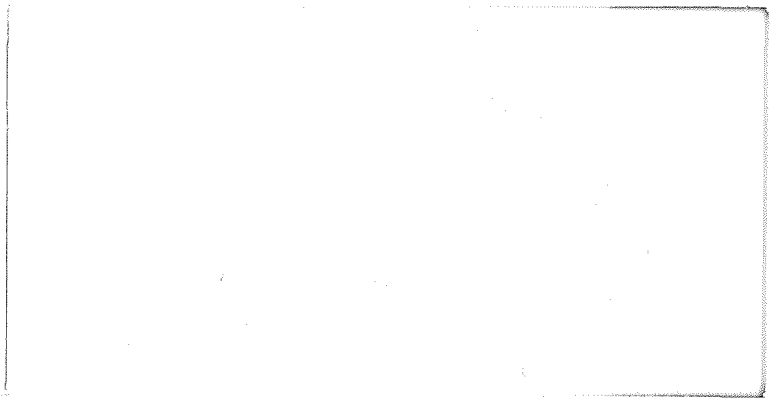

Amended (Pages 8 + 12)
20.4.82

Design Parameters and Model Testing for Bencat II

A.R. Packwood

April 1982

Internal Document No. 157

DESIGN PARAMETERS AND MODEL TESTING FOR BENCAT II

1. INTRODUCTION

Bencat is a freefall device to operate on the deep ocean floor and record three components of velocity in the benthic boundary layer. Bencat II is to be a less ambitious design than Bencat I in that it will only record velocities at one level above the sea-bed. It has the additional requirement that the current sensing electro-magnetic (e-m) heads should as much as possible be protected from handling and deployment/recovery damage without impairing their function. The primary aim of Bencat II will be to test the sensors in the deep ocean environment, hence only 2 e-m heads will initially be fitted together with an Aanderaa rotor and vane to give mean flow comparisons and instrument drift correction. Having been deployed and performed its function on the sea-floor, the instrument should on command release ballast, separate from the sea-bed and make its way to the surface for recovery.

The purpose of this study is to determine an acceptable design for the structure and for the location of instruments, buoyancy and ballast. Also to estimate ballasting and buoyancy requirements to give reasonable descent and ascent velocities and sufficient stability when in position on the sea-floor. The specified design maximum near bottom current that the device should withstand is 0.8 m/s. Acceptable rise speeds are approximately 1 m/s and on descent perhaps slightly less, say 0.7 - 0.9 m/s, to avoid damage on impact with the sea-floor. Also the device should not have any strong tendancy to kite or spin in transit from the surface to the sea-bed and vice-versa. Consideration should also be given to safety in handling, protection of the release in the critical deployment phase and ease of recovery from the sea-surface.

2. DESIGN OF THE FRAME AND ELECTRONICS HOUSING LOCATION

It has already been proposed that the frame containing the instrumentation should be constructed using aluminium alloy HV30-WP standard tubing 48.4 mm.ϕ, 4.47 mm wall thickness (7 SWG). This has a weight in water of 1.09 kg/m (1.72 kg/m. in air) and is favoured because of its lightness and corrosion resistance. It is also proposed that a disposable tripod base be used as on Bencat I and Bathysnap. The advantages that this offers are, known release technology, existing designs available for fabrication and the disposable base concept eliminates pull out problems should the feet become covered in sediment. It also means that a clean parting of the frame and ballast is more easily achievable without danger of entanglement. For ease of recovery and to keep the sensor package out of the wave action zone when the device arrives at

the surface it has been proposed that the buoyancy be tethered to the frame with a strop perhaps 10 m. long. This has the added advantage of separating the rather bulky buoyancy from the measurement systems which should be uninfluenced by surrounding structure as far as is practical. The favoured buoyancy is Benthos 17 in. ϕ glass spheres which have a good reliability record to date. Some redundancy in the number of spheres required is desirable in case of failure but the cost of spheres is high so designs requiring large numbers of them are to be avoided. The remaining problems are to configure the frame, electronics, instruments and buoyancy so that the stability of the equipment during descent, ascent and its period on the bottom be maximised bearing in mind the considerations listed in the introduction, plus those of cost and ease of fabrication.

It is essential that the sensors be protected from damage during deployment and recovery, this however conflicts with the operational requirement that the sensors be unobstructed. The stated primary objective of this device is to test the sensors and associated electronics in the deep ocean environment. Operational requirements can be relaxed provided the sensors are unobstructed for some of the time while the instrument is in position. The problem comes in keeping the sensors within a framework and yet uninfluenced by flow distortion round it. This can be achieved by careful positioning of sensors but only for mean flows from restricted angles relative to the frame. The basic frame proposed by Steve Thorpe is sketched below.

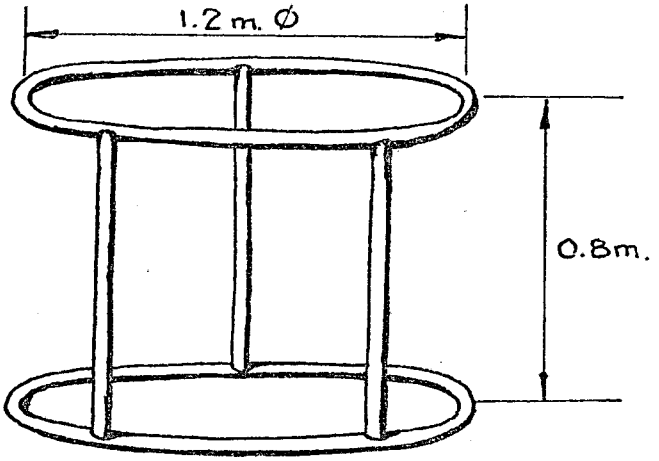

The instruments are to be optimally positioned within this frame and the electronics tubes placed above or below as seems best. Provision has to be made for the release and the attachment of the base and buoyancy.

The e-m current meter electronics, logging equipment and batteries will be stored in two 20 cm. ϕ by 66 cm. long tubes weighing 15.9 kg. each in water (36.7 kg in air). These together with the acoustic release, 15 cm. ϕ by 41 cm. long weighing 8.2 kg. in water (15.9 kg. in air), are to be mounted on the frame-work. Given that the acoustic release tube must be located at the top of the frame "looking" upward, there still remains three possible configurations for

the electronics tubes.

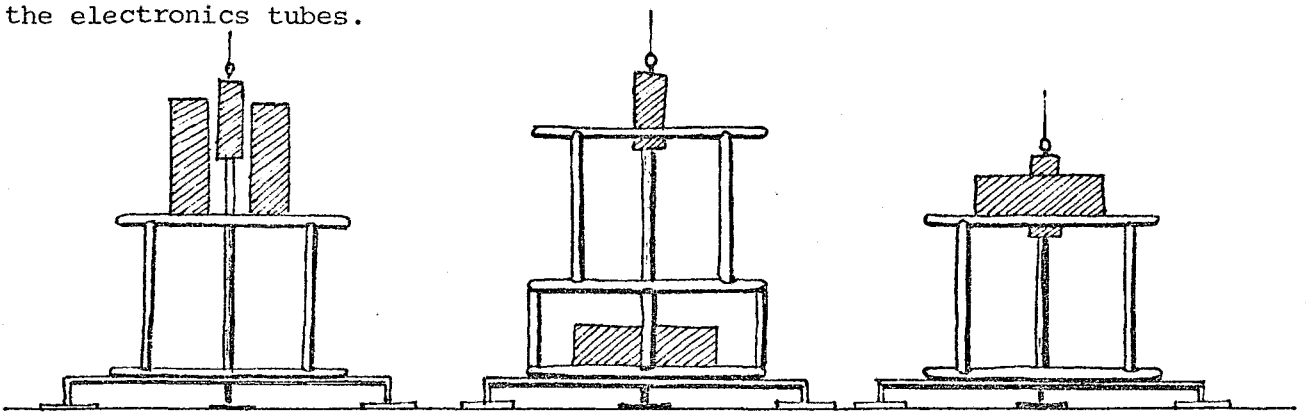

In (i) and (iii) the sensors will be 0.5 m off the seabed whereas in (ii) they will have to be at least 1 m off the bed in order to be reasonably well clear of the electronics tubes. The most critical condition that must be met is the resistance to overturning forces due to a horizontal stream while the instrument is in location. The shaded areas shown in the configurations above represent the maximum projected drag area for the tubes subjected to a horizontal current. Note that cylinders in tandem can give less drag than a single cylinder provided the spacing between centres is less than three diameters (see Horner (1958)), hence only one cylinder is shown in (ii) and (iii) as "worst cases".

It is clear that (i) is worse than (ii) or (iii) as far as drag forces are concerned due to the greater projected area and the overturning moment due to the drag of the tubes is less in (ii) than in (iii). However, the increased height of the frame and most importantly of the buoyancy tether point means that overall the overturning moments are higher in (ii) than in configuration (iii) which keeps the tether point low. Tether line forces will typically be an order of magnitude greater than the drag forces on the electronics tubes so consideration of the height of the tether point (together with the drag of the buoyancy) becomes more important. Hence configuration (iii) becomes the one adopted for further study. To accommodate this arrangement, a frame of design shown in fig. 1 is proposed. It is estimated that such a construction if fabricated entirely in aluminium alloy might weigh 40 kg. in water, 58 kg. in air. It is made up from 17.5 m. of tube and 3.5 m. of 10 cm. x 5 cm. channel section.

The disposable base also shown in fig. 1 is fabricated in steel and weighs 55 kg. in water, 64 kg. in air, without any additional ballast. The electronics tubes, acoustic release, current meters and release mechanism total another 55 kg. in water or 105 kg. in air. This gives an all up weight without any additional ballast of 150 kg. in water, 227 kg. in air.

To estimate the overturning moments assume that the base, in its worst

configuration, tends to pivot about its rearmost feet as in the sketch below

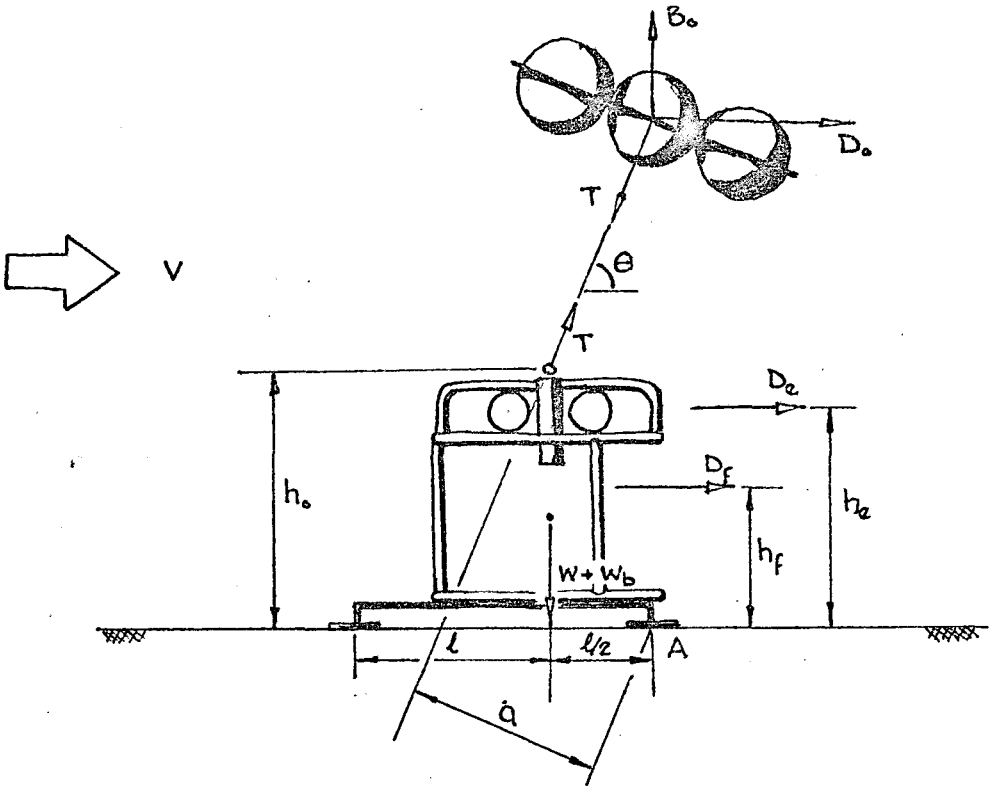

by taking moments about (A) it is found that...

$$Ta + D_e h_e + D_f h_f = (W + W_b)\ \frac{l}{2} \qquad (1)$$

where...

$$T = (B_o^{\,2} + D_o^{\,2})^{\frac{1}{2}}$$

$$a = \frac{1}{2\sin\theta} + (h_o - \frac{1}{2\tan\theta})\cos\theta$$

and...

$$\theta = \tan^{-1}\left(\frac{B_o}{D_o}\right)$$

B_o = nett buoyancy of float assembly

D_o = drag of float assembly

W = weight in water of instrument package + expendable base = 150 kg. (1st estimate)

W_b = weight in water of additional ballast (if required)

h_o = height off the bed of the tether point

... other variables are as defined in the sketch above. In this anslysis the lateral drag of the base and that of the tether wire have been ignored being judged not to significantly contribute to the overturning moment.

Assuming the framework to be constructed entirely of circular cylinders of

5 cm. and 2.5 cm. diameters, with total projected area 0.72 m^2, and drag coefficient 1.2 at typical Reynolds number of order 3×10^4, the drag D_f can be estimated assuming a velocity squared law giving

$$D_f \simeq 45\ V^2 \text{ kg}$$

For the electronics tubes in configuration (iii), the sum $\Sigma SC_D h_e$ for the tubes, assuming a similar drag coefficient acting on one electronics tube and the acoustic release gives

$$D_e h_e = 14\ V^2 \text{ kg.m}$$

Balancing the distribution of the structure of the frame the centre of area is at approximately $h_f = 0.7$ m from the sea-bed. Substituting this information into (1) gives

$$Ta + 45.5\ V^2 = \tfrac{1}{2}(W + W_b) \quad \text{(kg.m)} \qquad (2)$$

and

$$a = \frac{1}{2\sin\theta} + \left(1.3 - \frac{1}{2\tan\theta}\right)\cos\theta \ \text{(m)} \qquad (3)$$

since $l = 1$ m for the standard base and $h_o = 1.3$ m in configuration (iii).

3. BUOYANCY REQUIREMENTS AND CONFIGURATION

Since the weight in water of the structure to be recovered is approximately 95 kg, a minimum of six spheres is required. Each 17 in. sphere gives a nett buoyancy of 25.4 kg, therefore six spheres gives a nett buoyancy in ascent of approximately 50 kg, if all are intact. This figure depends on the weight of the structure holding the buoyancy together. Experience in using such free fall structures as the VACM camera tripod and Bathysnap suggests that 50 kg excess buoyancy is a reasonable figure. The recoverable structure on Bencat II is substantially larger than on previous devices however, so more buoyancy may be necessary to give the device an acceptable rise time. For the moment it is assumed that six spheres will be adequate. It is obviously desirable to minimise lateral drag whilst maintaining symmetry about the vertical axis for stability during the descent. There are a variety of possible configurations; one that has low lateral drag area has the spheres arranged in a ring of six. This presents a projected area of three spheres to the current stream but offers high drag to vertical motion. This may be desirable in the descent phase to reduce the fall velocity but it will also reduce the rise speed. Configurations having the spheres in a single horizontal row may possibly be oriented to give a projected area of only one sphere but this is difficult to arrange since free hanging devices tend to take on maximum drag attitudes in which they are often more stable. This would be very undesirable in this case.

The lateral drag coefficient of a single 17" Benthos sphere in a hard-hat is $C_D \simeq 1.0$ for flow parallel to the flange where C_D is based on the projected plan area $S = .255\ m^2$. These figures are as supplied by Benthos for trials at speeds in the range 20 - 50 cm/s. It will be assumed that the drag coefficient is similar at V = 80 cm/s. Because of the circular arrangement of the six spheres three will be shadowed and in tandem (3, 4 and 5 in the diagram below) so their drag is ignored. Also interference effects will tend to reduce the drag of spheres 2 and 6 since they are set just behind 1 and therefore in a turbulent stream which induces early flow separation.

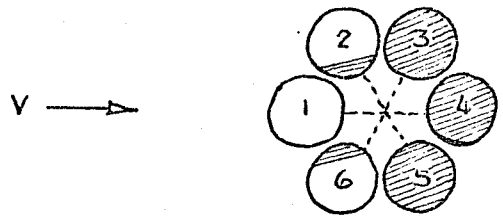

Suppose this effect reduces the drag on 2 and 6 by 10% then the drag of the buoyancy D_o becomes

$$D_o = 32V^2 \text{ kg.}$$

The buoyancy has to support its own supporting structure which will transfer the upthrust given by each sphere to a central tether point. The structure should also protect the spheres from mishandling and provide suitable lifting points. Supposing this structure to be fabricated from aluminium to provide the necessary strength for lifting and load transfer to the tether wire then the structure could weigh $\simeq$ 20 kg thus reducing the effectiveness of the buoyancy. With six spheres the nett buoyancy of this arrangement $B_o \simeq$ 130 kg.

In a current stream of V = 0.8 m/s from (1) and (3) the tether angle θ is 81.4^o giving a = 0.69 m. and T = 131 kg. So from (2) the necessary additional ballast weight W_b to just balance the overturning forces at V = 0.8 m/s is W_b = 88 kg. With the 6 sphere buoyancy arrangement discussed above, this gives nett weights in water of

on descent... 106 kg.
on ascent ... −37 kg.

It will of course be possible to add more ballast provided the resulting terminal velocity is not excessive, but it will not be possible to add buoyancy without adding an equal weight in water of ballast. Otherwise the overturning criterion is likely to be violated.

4. CALCULATED FREE FALL AND ASCENT VELOCITIES

4.1 DRAG OF BUOYANCY

The drag coefficient for a 17" Benthos sphere in a "hard-hat" type 204 SRO-17 with flow perpendicular to the flange is $C_D = 1.75$ based on the projected area of 0.255 m^2 as quoted by the Benthos company. If the spheres are arranged in a ring of six then the vertical drag due to the buoyancy will be not greater than that due to six individual spheres. This gives $SC_D = 2.68\ m^2$.

4.2 DRAG OF FRAME AND ELECTRONICS

Assuming the frame to be made up of circular cylinders and channel section and using standard drag coefficients as given by Hoerner (1958) the total SC_D value can be estimated.

	Projected area $S(m^2)$	C_D	SC_D
tubing	0.19	1.2	0.23
channel	0.23	2.0	0.46
electronics tubes	0.26	1.2	0.32
			$\Sigma SC_D = 1.01$

4.3 DRAG OF BASE

Similarly the base is made up of circular plates and "T" section beams which have known drag coefficients

	Projected area $S(m^2)$	C_D	SC_D
3 "T" section beams	0.105	→ ⊣ 1.65	0.17
1 disc 40 cm ϕ	0.126	1.2	0.15
3 discs 25 cm ϕ	0.147	1.2	0.18
			$\Sigma SC_D = 0.50$

4.4 THE ASSEMBLED STRUCTURE

It is assumed that the drag coefficients for the frame and buoyancy are similar on ascent and descent so that the totals for the entire assembly are

$$(SC_D) \text{ descent} = 4.19 \text{ m}^2$$

$$(SC_D) \text{ ascent} = 3.69 \text{ m}^2$$

Using the final weight estimates given in the previous section this gives terminal velocities for the package with six buoyancy spheres

$$\left.\begin{aligned} V \text{ descent} &= \left(\frac{W\text{nett}}{\Sigma SC_D} \times \frac{2g}{\rho}\right)^{\frac{1}{2}} = 0.70 \text{ m/s} \\ V \text{ ascent} &= \left(\frac{B\text{nett}}{\Sigma SC_D} \times \frac{2g}{\rho}\right)^{\frac{1}{2}} = 0.44 \text{ m/s} \end{aligned}\right\} \quad (4)$$

If it is possible to increase the number of spheres by one without significantly influencing the drag then for 7 spheres

$$V \text{ ascent} = 0.57 \text{ m/s}$$

and for 8 spheres with no additional drag penalty

$$V \text{ ascent} = 0.67 \text{ m/s}$$

For these latter cases only the ascent velocity is shown because from the overturning calculation it has been shown that a minimum nett weight of about 106 kg is required to maintain stability in a current stream of 80 cm/s. This is the value obtained with the 6 sphere configuration with 88 kg additional ballast on the base. If more spheres are added then an equal amount of ballast is also required to maintain the minimum nett weight of 106 kg in sea water, so the descent velocity remains unchanged provided the drag is not significantly increased.

5. OPTIMAL POSITIONING OF THE SENSORS WITHIN THE FRAMEWORK

The problem is to position the three sensors so that wake interference from the surrounding and supporting structure is minimized. While keeping the heads inside the structure this will only be possible in a limited azimuth window within which all three sensors will be clear at the same time. Ideally the sensors should be close together so that they sample over a small volume - but then mutual flow interference between sensors and their supports becomes a problem. To investigate this a simple wake model due to Schlicting (1955) was used which gives the wake spreading behind a circular cylinder

$$\frac{y}{d} = \left(C_D \frac{x}{d}\right)^{\frac{1}{2}}$$

where y is the wake boundary measured from the centre-line, x is the downstream distance along the centre-line of the wake, d is the diameter of the cylinder and C_D its drag coefficient.

Three possible locations for the e-m heads were selected and using the above model the wake boundary lines were drawn from vertical frame members and sensor supports. Flow directions for which the boundaries interfered with each of the sensors in the various locations were then drawn onto a scale diagram. So for each instrument sectors in which some flow interference could be expected were constructed. These interference sectors and the selected instrument locations are shown in fig. 2. For the two e-m heads to be open to the flow then the combined open window angle ψ is twice the smallest angle to the horizontal shown on the diagram. Thus for the various locations

e-m head location	ψ^{o}
1	140
2	70
3	68

Location 1 is obviously best for the e-m heads. With the heads in this position the mechanical current meter can be moved from location 4 to 5 which does not restrict the window open to the e-m heads but increases the open window of the mechanical c.m. to 134^{o}. Thus with e-m heads in locations 1 and mechanical c.m. at 5 the overall unobstructed azimuth window is 134^{o}. The device therefore has a preferred operational direction. For flows from this direction, right to left on fig. 2, the instrumentation tubes offer minimum drag and the tripod base is aligned to give maximum resistance to any overturning moment. Thus the frame has its greatest stability in this orientation. If in general flow is omni-directional then the instrument may only be expected to sample unobstructed flow for approximately $\frac{1}{3}$ of the time of its deployment. This cannot be avoided unless more sensors are fitted.

5. MODEL SCALING

Apart from the obvious model scaling criterion of geometric similarity the other major requirement is that drag to weight ratios for the model and full scale device be similar. This is in order that observed attitudes in free fall or in a current stream may be preserved under the scaling. Due to the limited available facilities it was decided that the model scale experiments will be carried out in fresh water so apart from small differences the fluid density and viscosity will be similar. The drag force may be described generally by

$$D = \tfrac{1}{2} \rho V^2 G d^2 C_D \qquad (5)$$

where ρ = fluid density, V = fluid/body velocity, G = geometric similarity parameter, d = representative dimension of the body and C_D is the drag coefficient. If (5) represents the drag of the full-scale device then at model scale

$$D' = \tfrac{1}{2}\rho V'^2 G s^2 d^2 C_D' \qquad (6)$$

where d' = sd, s being the scale factor, $\rho = \rho'$ by similar fluids and G = G' by geometric similarity where dashes indicate model scale variables. Thus for similar drag to weight ratios from (5) and (6) it is found that

$$\frac{W'}{W} = \left(\frac{V'}{V}\right)^2 \cdot \left(\frac{C_D'}{C_D}\right) s^2 \qquad (7)$$

If the weights are scaled geometrically, which significantly eases the problems of model manufacture, such that

$$\frac{W'}{W} = s^3$$

then (7) becomes

$$\frac{V'}{V} = \left(\frac{sC_D'}{C_D}\right)^{\frac{1}{2}} \qquad (8)$$

It would be convenient if it could be arranged that $C_D' = C_D$ since this would simplify (8). Unfortunately this requires Reynolds number similarity which conflicts with (8) since by Reynolds number similarity

$$\frac{V'}{V} = \frac{1}{s}$$

if the fluids are similar. However, drag coefficients for simple shapes like cylinders, circular plates and spheres exhibit a range of Reynolds numbers over which the drag coefficient remains sensibly constant. The range of Reynolds numbers is

$$10^3 < Re < 3 \times 10^5$$

i.e. within the turbulent flow regime but before the flow becomes super-critical, see Hoerner (1958). Provided then that Re and Re' lie within this range the drag coefficients will be similar and (8) reduces to

$$\frac{V'}{V} = s^{\frac{1}{2}}$$

Since the framework and base are relatively open structures, the relavant Reynolds number will be that based on the size of individual components i.e. tube diameter, diameter of plates or of the buoyancy spheres, thus typical Reynolds numbers at the design speed of 0.8 m/s are 2.7×10^5. It is apparent that at this speed quite a wide range of scale factors are acceptable for it is easily shown that

$$Re' = s^{3/2} Re$$

Quite small values of s are possible that maintain $Re' > 10^3$. For the typical full scale Reynolds number of 2.7×10^5 the smallest scale factor is 1/40. But at lower full scale velocities, say 5 cm/s, the minimum value for s increases to $\frac{1}{6}$. It was therefore decided that s should take the value of $\frac{1}{4}$. This is a convenient figure since it gives $V' = V/2$ and $W' = W/64$, but it also enables quite a wide range of flow conditions to be investigated with more confidence.

7. DESCRIPTION OF THE MODEL AND EXPERIMENTS

The model is $\frac{1}{4}$ full scale and was designed to weigh approximately 1/64 of the full scale weight. Photographs of the model frame and assembled components are shown in fig. 3. Details of the weights of the components full scale, at model scale and as measured at model scale are given in Table 1. The buoyancy was made up of 5½" diameter rigid plastic nett floats with a PVC collar machined to simulate the flange of the Benthos hard-hats. The floats give considerably more buoyancy than required by the scaling so an additional amount of ballast was necessary. The assembled buoyancy structure and ballast are shown in fig. 4. Note that the mechanical current meter on the model is not in its optimum position suggested in section 5 but is placed in a central location for convenience in model manufacture. Because of the limited combination of brass weights available for ballasting, the trimming weights for individual components are in some error. These errors largely cancel when the structure is fully assembled so that the final assembly is over ballasted by 76 gm in its descent configuration and 221 gm (14 kg full scale) when the base is removed for the ascent. Errors of this sort can be tolerated since it is the drag coefficient of the structure that the tests will give which can be used to predict the full scale behaviour at the corrected weights, provided they are not very much different.

Two series of tests were carried out. The first was a free fall/ascent test to determine the model stability and velocity on descent and ascent. The second was a series of overturning tests to determine the stability of the device on the sea-floor to lateral flows and the limiting current that the instrument could withstand.

7.1 FREE FALL TESTS

The drop tests were carried out at H.M.S. Dolphin, submarine escape training tank, Gosport. The tank is ≈ 30 m deep and 5 m in diameter

and is filled with chlorinated fresh water kept at ≈ 20°C. A team of free swimming divers was employed to drop, time and retrieve the model on each trial. The model was assembled with the buoyancy separated from the frame on 2.5 m of nylon chord. With the frame suspended underneath the buoyancy was held at the surface and released. Divers positioned at depths of 5 m and 15 m signalled to the surface when the base passed the depth mark which was painted on the side of the tank. Observers at the surface were able to record the travel time over the 10 m interval over which it was assumed that the velocity was constant. A picture of the model on a trial descent is shown in fig. 5. For the ascent the model with base removed was released from a diving bell at about 20 m depth and the same method was then used to time the ascent. Each test was repeated once, or twice if results were not found to agree, and two independant observers with separate stop watches were used to record the time between signals. To quickly change the weight of the model in water the buoyancy arrangement was designed so that a 7th pre-ballasted sphere could be rapidly screwed onto the buoyancy array. This sphere was mounted in the middle of the array and did not have a flange glued onto it so that the drag would not be much influenced. The weights in fresh water for the model in its various configurations are given on Table 1. The results of the tests are given below.

		model scale			full scale		
		Weight W' (gm)	Velocity V'_τ (cm/s)	$(S'C_D)$ (m^2)	Weight W (kg)	Velocity V_τ (cm/s)	(SC_D) (m^2)
6 floats	descent	1700	45	0.165	109	90	2.64
	ascent	-398	22	0.161	-25.5	44	2.58
7 floats	descent	1290	39	0.165	82.6	78	2.64
	ascent	-816	29	0.193	-52.2	58	3.09

where the full scale values are given by (see section 6)

$$W = 64W'; \quad V_\tau = 2V'_\tau; \quad SC_D = 16S'C_D$$

At the estimated full-scale weights derived by calculation for the full scale device the terminal velocities as given by (4) using SC_D values derived from the experiments are

	W(kg)	V_τ (cm/s)		V_τ (cm/s)	[obtained by calculation from section 4]
6 spheres	106	87	descent	70	
6 spheres	-37	52	ascent	44	
7 spheres	-62.4	62	ascent	57	
8 spheres	-87.8	74	ascent	67	

It is clear that the calculations of section 4 overestimated the value of ΣSC_D and consequently underestimated the terminal velocities.

7.2 OVERTURNING TESTS

To test the stability of the model when it is in position on the sea floor a ground board was slung beneath the tow carriage on the Wormley wave/tow tank facility. This device was previously constructed by Lampitt & Griffiths (1980) and is described in their paper. A diagram of the ground board and supporting structure is given in fig. 6. A fine mesh plankton net and four boundary layer trips of frayed netting are used to artificially thicken the boundary layer on the board. The natural boundary layer would otherwise be very thin over the working area which is approximately 1 m from the leading edge of the board.

Boundary layer velocity profiles were measured using a miniature discus shaped e-m head, also shown in fig. 6. A similar head is described in Griffiths (1979). The head is capable of giving two components of velocity spacially averaged across the electrodes which are 25 mm apart. The e-m head is mounted on 30 cm of ¼" tube which was fixed into a length of streamlined aluminium strut. The strut was clamped in a block on the carriage which could position the head at any point above the board. The strut was calibrated to give the height of the sensor head above the ground plane. The signal from the sensor was filtered to give a mean velocity signal which was subsequently processed and recorded on the Camac/HP 26 47A computer on the tow carriage. The sampling rate was 5 Hz and most of the recordings were of about 20 sec duration. The electrodes were aligned to measure flow parallel and normal to carriage motion. The head was calibrated by raising it 90 cm above the board ($\sim$ 50 cm below the free surface) well out of the boundary layer and driving the carriage at a range of speeds between 0 - 50 cm/s accurately recording carriage speed when conditions were steady.

Velocity profiles were taken at two stations on the board at 1 m and 1.32 m from the leading edge on the centre line. This was just ahead and just aft of the position where the model frame was to be situated. A nominal tow carriage velocity of 40 cm/s was used in obtaining the velocity profiles since at model scale this corresponded to the maximum near bottom current given in the specification. For all of the runs at the various probe heights and locations the average carriage speed was u_c = 39.28 cm/s. Details are given in Table 2. The velocity

profiles are plotted in fig. 7, these indicate that the boundary layer is between 20 - 30 cm thick at these locations. This corresponds well with the scaled thickness of the logarithmic layer ($\sim$ 1 m full scale $\therefore$ 25 cm at model scale) suggested by Wimbush & Munk (1968). Plotting the profiles on a logarithmic scale indicates the extent of the logarithmic layer on the model ground plane. The slope of the curve in this region, ignoring the point nearest the ground and those outside the boundary layer, enables the friction velocity u_* to be estimated. Choosing the von Karman constant $\kappa \simeq 0.4$ then from

$$\frac{u}{u_*} = \frac{1}{\kappa} \ln\left(\frac{yu_*}{\nu}\right) + c$$

where c is a constant and ν the kinematic fluid viscosity, we find $u_* = 9.12$ cm/s for $u_c = 39.28$ cm/s. This value is very large compared with that previously measured in the ocean where u_* values of about 0.1 cm/s are expected, see Wimbush & Munk (1968). Hence although the boundary layer thickness is reasonably represented on the ground board the structure of the boundary layer is very different. It is thought that this is because of the very limited extent of the ground board which does not give the boundary layer long enough to develop and reach an equilibrium state. At lower velocities the situation is improved however. From the results of Lampitt & Griffiths (1980) velocity profiles at similar position on the same board for $u_c = 20$ cm/s gives $u_* = 1.67$ cm/s.

Fig. 8 shows the model in position on the ground board - the underwater T.V. camera can be seen in the background. Injecting dye into the boundary layer through an upstream capillary tube with and without the model in position showed that there was no observable influence of the structure on the flow in the vicinity of the heads. Fig. 9 shows multiple dye traces taken from an underwater T.V. recording of the dye injection experiments at a carriage velocity of 20 cm/s. This picture was obtained by superimposing individual dye traces taken from the 20 sec long recording. It thus portrays the envelope of the dye traces which are very similar both with and without the model in position. The greater density of traces in both cases shows fluid being entrained into the depths of the boundary layer. These are of doubtful value since the structure of the oceanic boundary layer will be very different but they perhaps lend some confidence to the design of the frame.

The main purpose of the moving ground experiments however was to determine the in situ stability of the chosen configuration subject to high speed currents. The fully assembled structure complete with the six buoyancy spheres was lowered onto the ground plane at the location shown in fig. 6. The tow carriage was slowly accelerated until the model was observed to move and the speed at which this occurred was recorded. With the six sphere buoyancy assembly the model moved at a carriage speed of between 41 - 44 cm/s. The model was observed to slide and hop downstream as if it were being lifted by the action of the current. Fig. 10 shows the model frame being towed on the ground board at 40 cm/s with the carriage moving from left to right in the picture. The dye capillary tube can be seen upstream of the model. The model was next oriented so that one of the tripod feet pointed into the stream and the rear feet were restrained from sliding using heavy steel wedges. The full-scale device has pegs on the bottom of the feet which sink into the sediment to give some anchorage against sliding. So the wedges were placed to prevent sliding but allow tipping. Repeating the experiment indicated that the leading foot lifted off the ground board at a tow speed of 42 - 43 cm/s. The frame did not tip right over but the front foot appeared to hang in the stream lifting further off the ground as the speed was increased. This behaviour again indicated that lift as well as drag was responsible for the separation from the bottom. The primary source of lift comes of course from the buoyancy but this is hydrostatic in origin. However in a current stream the buoyancy ring assumes an angle of incidence that may give rise to some hydrodynamic lift. The plane of the ring of spheres remains normal to the tether line which is swept back by the drag on the buoyancy assembly.

7.3 BUOYANCY LIFT AND DRAG

A further set of experiments was devised to measure the tether rope angle and tension for a range of currents 0 - 50 cm/s. The scheme of the experiment is shown in fig. 11. To provide comparative figures two buoyancy arrangements were considered (also shown in fig. 11). The backward drift of the buoyancy in the current was measured using a sight-bar which gave the downstream displacement from the zero current position of a point sighted on the buoyancy. The tension was measured using a strain gauge balance which was calibrated before and after the experiment. The results are given in Table 3. Here l is the downstream drift of the sighted point on the buoyancy and h the height of the sight point above

the pulley centre line at u_c (carriage speed) = 0. At speeds lower than those shown in the table for the respective configurations the tension carrying cable was fouled by the buoyancy structure so only comparitively high values of u_c are shown. It is clear from the results that at current speeds greater than 40 cm/s at model scale the "3 on 3" configuration is much better than the "6 in a ring" configuration both in terms of tether angle and tension. At 40 cm/s the drag coefficients for the 2 configurations are similar but at higher speeds the drag coefficient for the "6 in a ring" arrangement is approximately 1.8 times that of the "3 on 3". The negative lift coefficients are difficult to explain and may be due to friction in the pulley - however the influence of lift is clearly seen in the "6 in a ring" results at the higher tow speeds. Drag coefficient is obviously a function of angle θ and the simple estimates of section 3, though giving a reasonable low speed estimate of SC_D are inappropriate at higher speeds where the angle θ becomes appreciable.

8. IMPLICATIONS OF USING THE "3 ON 3" BUOYANCY ARRANGEMENT

The ballasting requirements of the device with the "3 on 3" buoyancy assembly will be similar to that previously calculated with the "6 in a ring" arrangement. This is because the drag coefficients are similar at the model design speed of 40 cm/s (80 cm/s full scale) $SC_D \simeq 0.58$ cf. 0.61 previously estimated. The new arrangement offers some additional advantages in handling and the structure containing the spheres may be simplified thus reducing its weight. Also the terminal velocities on descent and ascent are likely to be increased which would save ship time. Using the drag estimates of section 4 and the measured drag in the free fall experiments it is possible to set some bounds on what the terminal velocities may be but without repeating the experiments it is difficult to be precise. Assuming the buoyancy drag to be half that calculated in section 4 then using the same theoretical estimates for the remaining structure the velocities become

descent	84 cm/s
ascent	54 cm/s

This gives a lower bound to the terminal velocities for the drop tests have already shown that the theoretical SC_D values for the structure with a "6 in a ring" buoyancy arrangement were over estimated by a factor of $\simeq 1.5$. If this same factor is applied to the new theoretic estimate with the "3 on 3" arrangement then the following velocities are obtained

descent	106 cm/s
ascent	66 cm/s

It is hoped that the true full-scale value will lie somewhere between these two empirical estimates.

9. CONCLUSIONS

The tests and calculations have provided a basis from which the ballasting and terminal velocity estimates for Bencat II can be made.

At this stage a small aluminium frame is suggested to protect the sensors as in fig. 1. The logging/battery tubes are mounted horizontally above the frame to reduce lateral drag which is a severe constraint if the device is to withstand currents of 80 cm/s. The instruments record at a height of 50 cm off the sea-bed and if grouped as suggested in section 5 will have an unobstructed azimuth window of approximately 134^{o} as shown in fig. 2.

Assuming component weights shown in table 1, the recommended additional ballast weight is 88 kg in water to prevent the instrument overturning in a 80 cm/s current. The buoyancy selected is 6 x 17" Benthos glass spheres stacked 3 on 3, separated from the sea-bed unit by a 10 m (or more) wire strop. Terminal velocity estimates for the device are between 84 and 106 cm/s on descent and 54 and 66 cm/s on ascent. Greater precision is not possible without further free fall testing with the buoyancy arrangement finally suggested. From the towing tests and dye studies there is no evidence of any severe flow distortion in the region of the sensors due to the presence of the surrounding structure.

The theoretical estimates of required ballasting were well supported by the overturning tests which indicated that the device would move in a current stream of 84 cm/s. Suction forces on the feet might improve this performance if the device is deployed in regions of soft sediment where some settlement is expected. The calculated terminal velocities underestimated the model test velocities by approximately 23% both on descent and ascent. Hence the reason for the range of velocities given above to cover this uncertainty for the device with the modified buoyancy arrangement not tested at HMS Dolphin.

The author is grateful for the assistance of Lt. Comms Charter and Russell and the staff of the Submarine Escape Training Tank, HMS Dolphin for their assistance in carrying out some of the experiments.

Important An addendum is attached which gives updated estimates of component weights and how this influences buoyancy, ballasting and terminal velocity.

REFERENCES

Griffiths G. (1979) The effect of turbulence on the calibration of electromagnetic current sensors and an approximation of their spatial response.
I.O.S. Internal Document 68.

Hoerner S.F. (1958) Fluid Dynamic Drag.
pub. by author.

Lampitt R.S. & Griffiths G. (1980) The influence of a sea-bed structure (Bathysnap) on near bottom currents.
I.O.S. Internal Document 110.

Schlicting H. (1955) Boundary Layer Theory.
pub. Pergamon Press.

Wimbush M. & Munk W. (1968) The benthic boundary layer.
In: The Sea Vol. 4: 731-758, ed. A.E. Maxwell.

Table 1

Component	Full scale	$\frac{1}{64}$ full scale	Measured model scale		Trim (brass)			
	Water (kg)	in water (gm)	Air (gm)	Fresh water (gm)	required		actually added in experiment	
					water	air	in air	in water
Frame + electronics instruments	95	1480	2459	1365	115	131	40	35
Base & ballast: base 55, ballast 88 } 143	143	2234	1891	1700	534	595	450	395
1 x 17" sphere	-25.4 x 6 = -152.4	-397	-	-784	387	440	433	380
Buoyancy structure	≈ 20	313	716	624	-311	-354	-	
Fully assembled								
6 spheres: descent	106	1656	-	1695		3012	3088 - over ballasted by ≈ 76 gm	
6 spheres: ascent	-37	-578	-	-400		2417	2638 - over ballasted by ≈ 221 gm	
		7 spheres fully assembled	-	1290 descent				
			-	-816 ascent				

Table 2

Run	y (cm)	u_c (cm/s)	u (cm/s)	u/u_c	ln (y)	
1	5	0	0	0	1.61	132 cm from L.E.
2	5	39.37	16.8	0.427	1.61	
3	10	39.24	22	0.561	2.30	
4	15	39.14	31.8	0.812	2.71	
5	20	39.04	36.9	0.945	3.00	
6	25	38.93	37	0.95	3.22	
7	30	39.96	37.1	0.952	3.40	
11	4.1	0	0	0	1.41	100 cm from L.E.
12	4.1	39.7	11.2	0.282	1.41	
13	9.1	39.34	20.8	0.529	2.21	
14	14.1	39.27	32.7	0.833	2.65	
15	19.1	39.73	38.6	0.972	2.95	
16	24.1	39.39	37.5	0.952	3.18	
17	29.1	39.22	37.7	0.961	3.37	

Table 3 Comparative buoyancy lift/drag study

(1) "3 on 3" h = 84 cm

u_c (cm/s)	l (cm)	θ^o	T (kg)	D (kg)	L (kg)	SC_D (m^2)	SC_L (m^2)	full scale SC_D (m^2)
30	10.5	7.2	1.71	.21	-.07	.046	-.015	.736
40	15.2	10.4	1.58	.29	-.22	.036	-.027	.576
50	22.8	15.7	1.66	.45	-.17	.035	-.013	.56

(2) "6 in a ring" h = 88 cm

u_c (cm/s)	l (cm)	θ^o	T (kg)	D (kg)	L (kg)	SC_D (m^2)	SC_L (m^2)	full scale SC_D (m^2)
40	14	9.2	1.69	.27	-.1	.033	-.012	.53
45	26.9	17.8	2.06	.63	.19	.061	.018	.98
50	34.2	22.9	2.16	.84	.22	.066	.017	1.06

ADDENDUM

REVISIONS DUE TO DESIGN CHANGES

(i) REVISED WEIGHTS OF COMPONENTS IN WATER

	kg	lb
Frame: now to be manufactured from 8 SWG Al. tube	25	55
Buoyancy structure	18	40
Electronics and instruments (unchanged)	55	121
Total weight of recoverable parts - in water	98 kg	216 lb
Base: in heavier gauge steel	91	200
Additional ballast weights 1" thick steel plate - each to be added to base to increase ballast	12	27

(ii) BUOYANCY

Five spheres would be just sufficient to bring back the recoverable structure. In the event of a failure of one of the spheres, the buoyancy loss is 36 kg allowing for the weight of the glass of the damaged sphere. The remaining four spheres do not have sufficient lifting power to bring the instrument back so six spheres are still required to give a redundancy of one. Benthos suggest that a minimum separation of 1 diameter between spheres is advisable to prevent multiple failure in the event of one sphere imploding at depth. This constraint is difficult to overcome without making the buoyancy unwieldly to handle and of increased drag which would reduce the in-situ stability. Because of the high reliability to date of Benthos spheres, this latter constraint is to be ignored in favour of a more compact design.

nett weight on descent	$(37 + W_b)$ kg	
	$(73 + W_b)$ kg	with one sphere failed
nett buoyancy on ascent	54 kg	
	16 kg	with one sphere failed

(iii) ADDITIONAL BALLAST W_b TO PREVENT OVERTURNING IN 80 CM/S CURRENT

Lateral drag coefficient of "3 on 3" buoyancy arrangement

$SC_D = 0.6$ m² @ 80 cm/s - based on model test @ 40 cm/s

gives $D_o = 20$ kg @ 80 cm/s.

nett upthrust of buoyancy assembly $B_o = 134$ kg

strop tension T = 135 kg angle to flow $\theta = 81.5^{o}$

With the revised estimate for W = 171 kg (2) becomes

$$W_b = 2(Ta + 45.5V^2 - 85.5)$$

and using (3) $W_b = 73$ kg (160 lb)

This is equivalent to adding 2 ballast weights to each foot.

With this additional ballast the nett weight on descent becomes

W nett = 110 kg

146 kg with 1 failed sphere.

(iv) TERMINAL VELOCITY ESTIMATES

Using the same empirical criteria as discussed in section 8 gives -

		$SC_D(m^2)$	V_T(cm/s)	V_T(cm/s) with one sphere failed
min. theoretical	descent	2.9	85	98
estimate for velocity	ascent	2.4	65	36
max. empirical estimate	descent	1.8	108	124
based on experiment	ascent	1.6	80	44

FIG. 1 SKETCH OF FRAME AND DISPOSABLE TRI-POD BASE

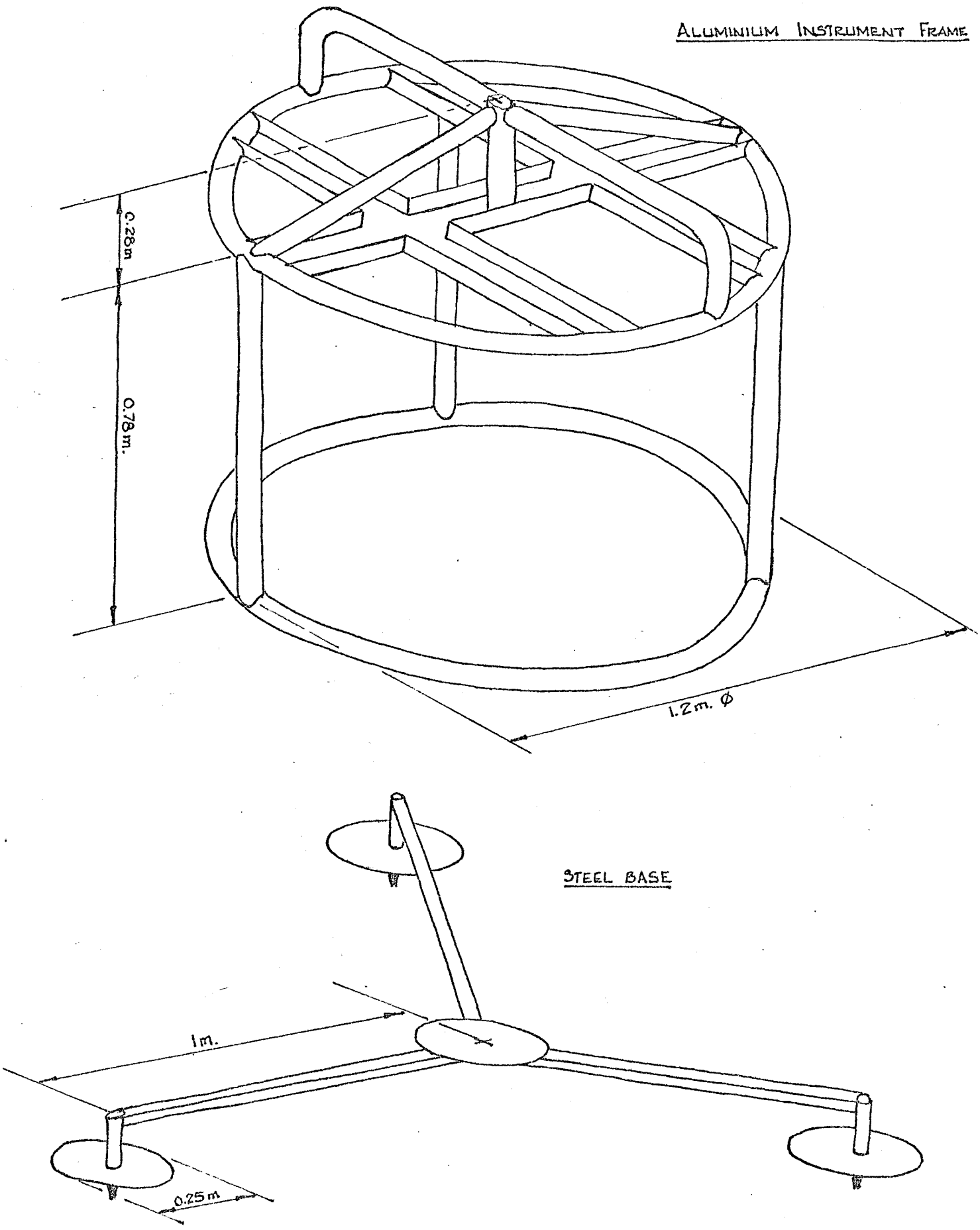

FIG. 2 OPTIMIZING SENSOR LOCATION FOR MAX. CLEAR AZIMUTHAL VIEW

E-M. CURRENT METERS A SINGLE PAIR ARRANGED AT 90°

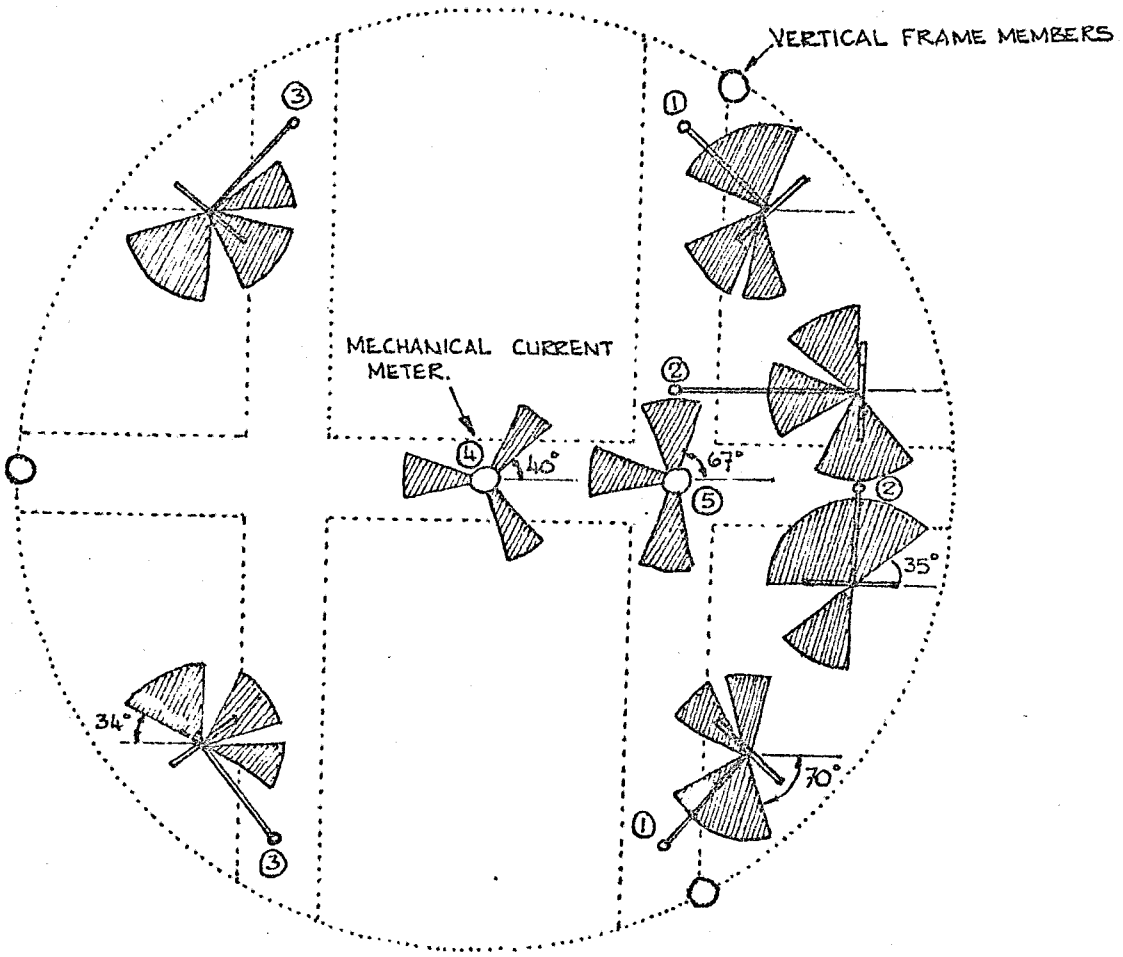

SHADED SECTORS SHOW DIRECTIONS FROM WHICH FLOW IS DISTURBED BY WAKES FROM STRUCTURE MEMBERS OR NEARBY SENSORS.

BEST LOCATIONS SHOWN ARE ① FOR E-M. HEADS : ⑤ FOR MECHANICAL C.M.

FIG. 3 MODEL FRAME AND BASE WITH INSTRUMENTS AND ELECTRONICS HOUSINGS.

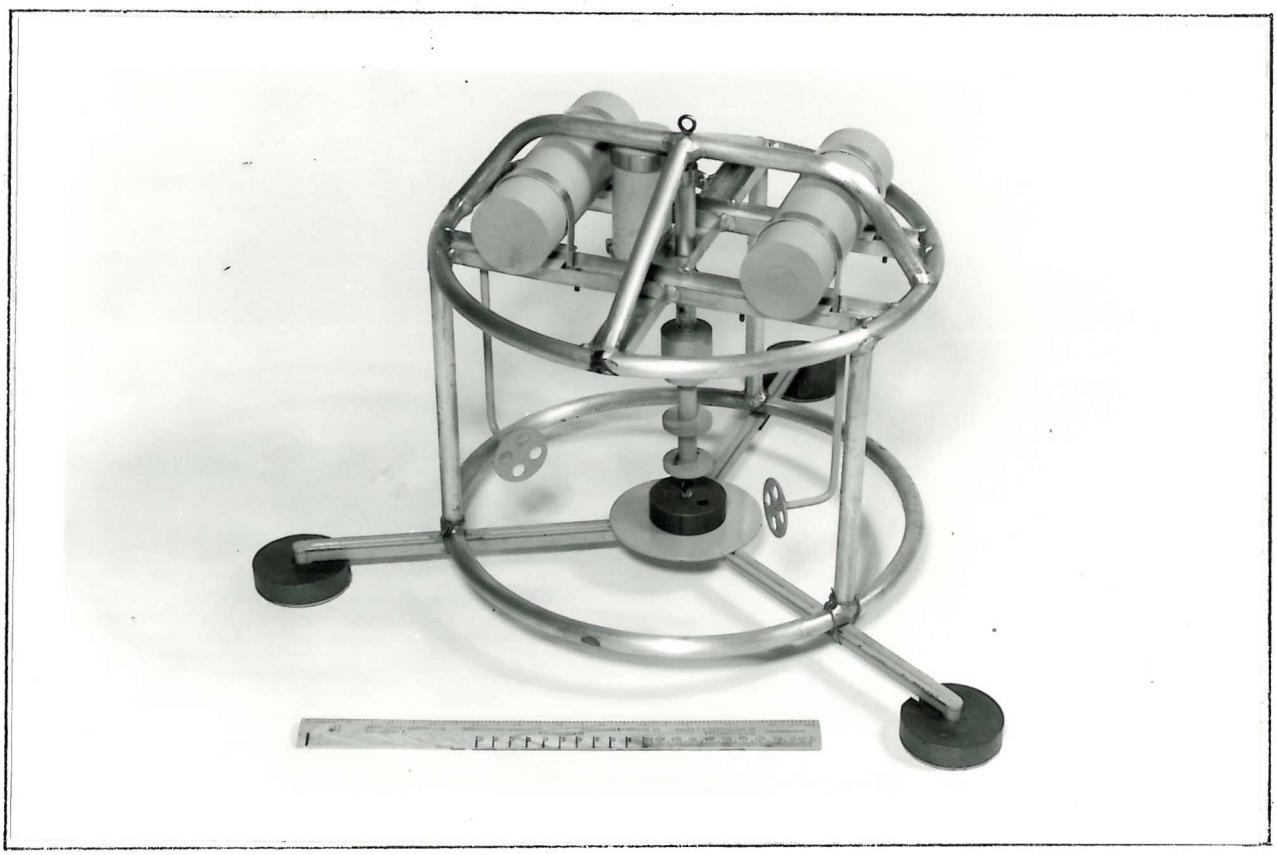

FIG. 4 MODEL BUOYANCY ASSEMBLY AND BALLAST

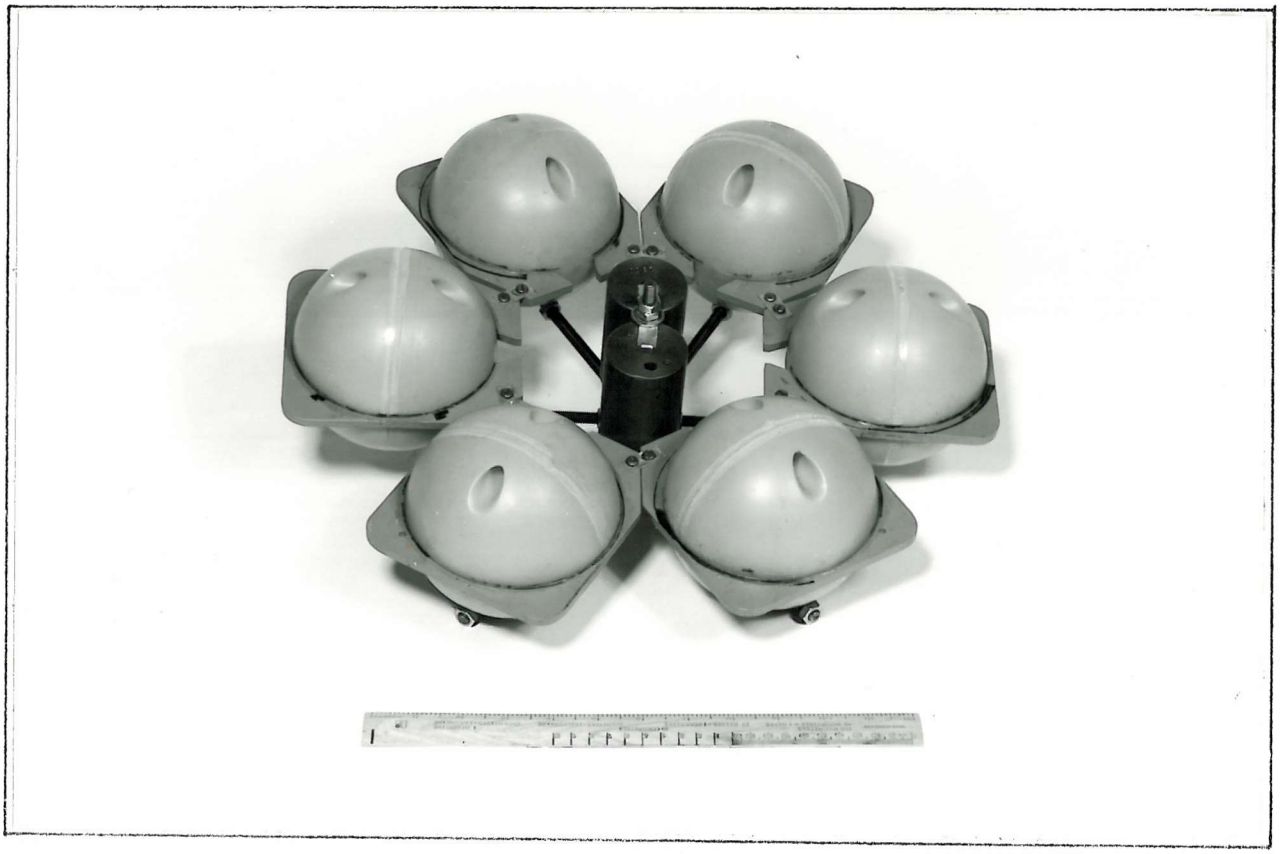

FIG. 5 FREE FALL MODEL TEST AT H.M.S. DOLPHIN.

FIG. 6. DETAILS OF GROUND-BOARD INSTALLATION.

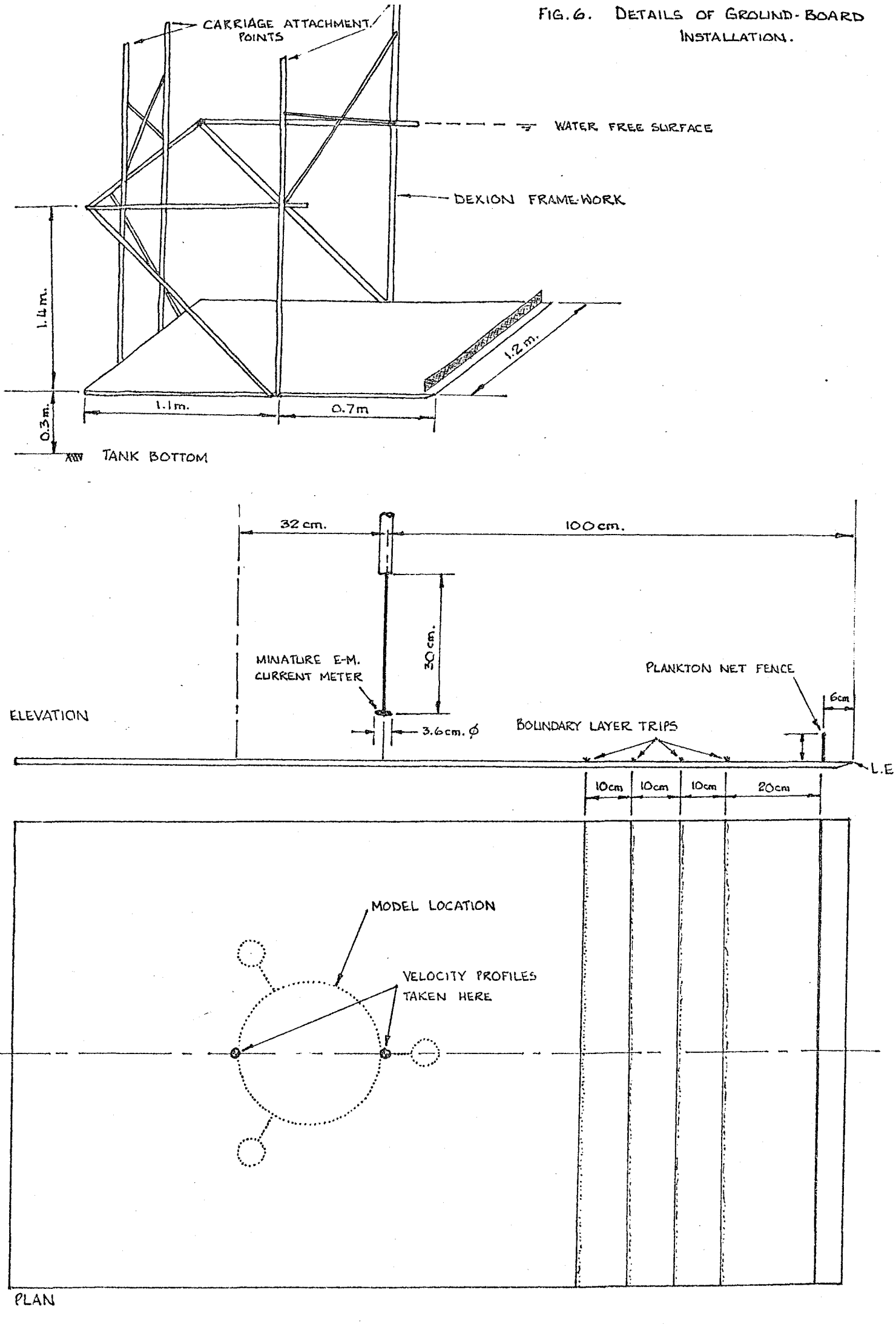

FIG. 7 GROUND-BOARD VELOCITY PROFILES

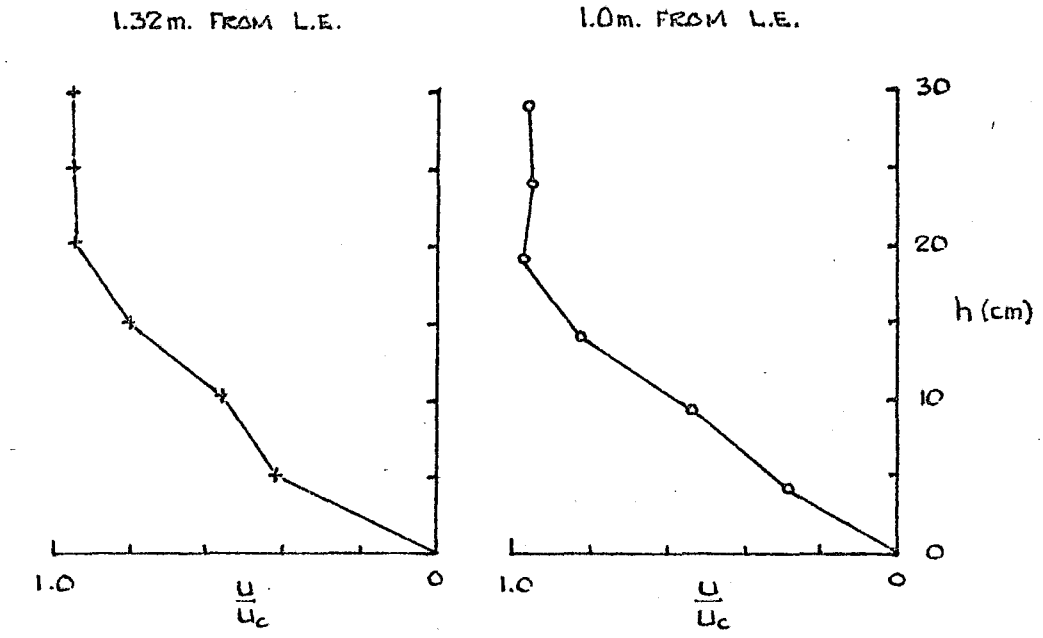

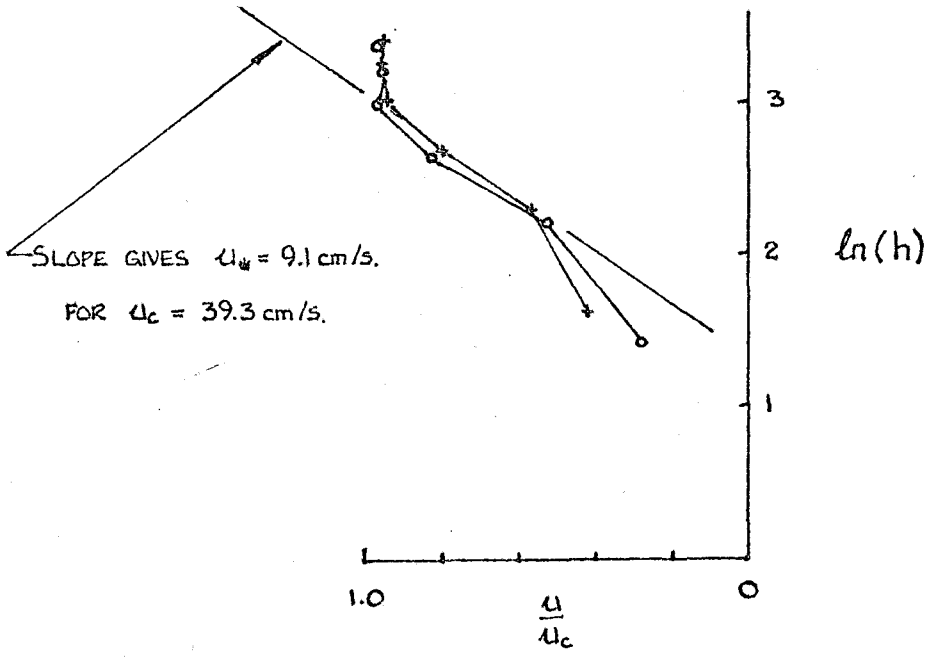

FIG. 8 MODEL SITTING ON THE GROUND BOARD IN THE TOW-TANK
GROUND-BOARD STATIONARY

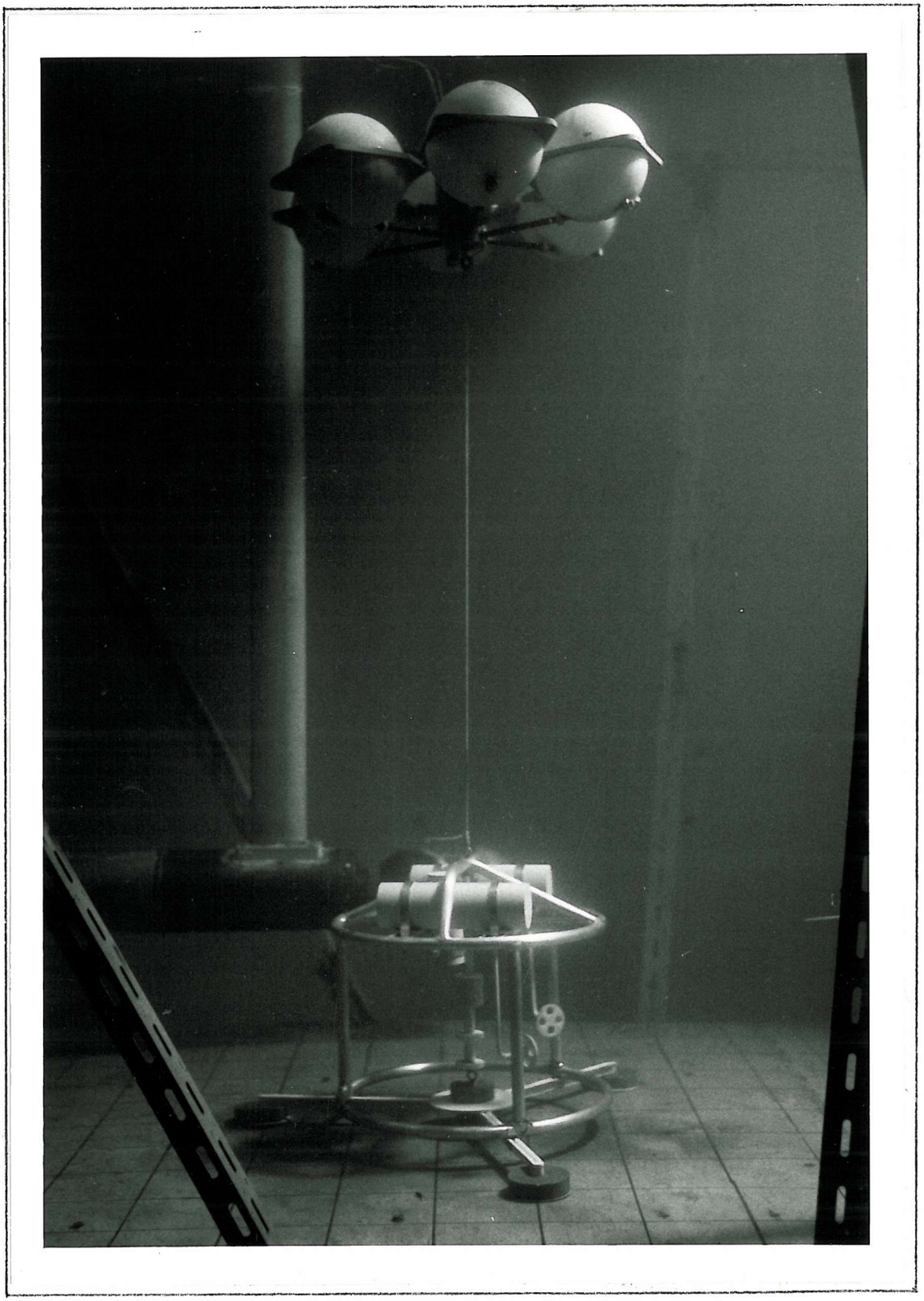

FIG. 9 MULTIPLE DYE TRACE OVERLAYS FROM T.V. RECORDING OF THE MOVING GROUND BOARD EXPERIMENT

GROUND BOARD SPEED 20 cm/s.

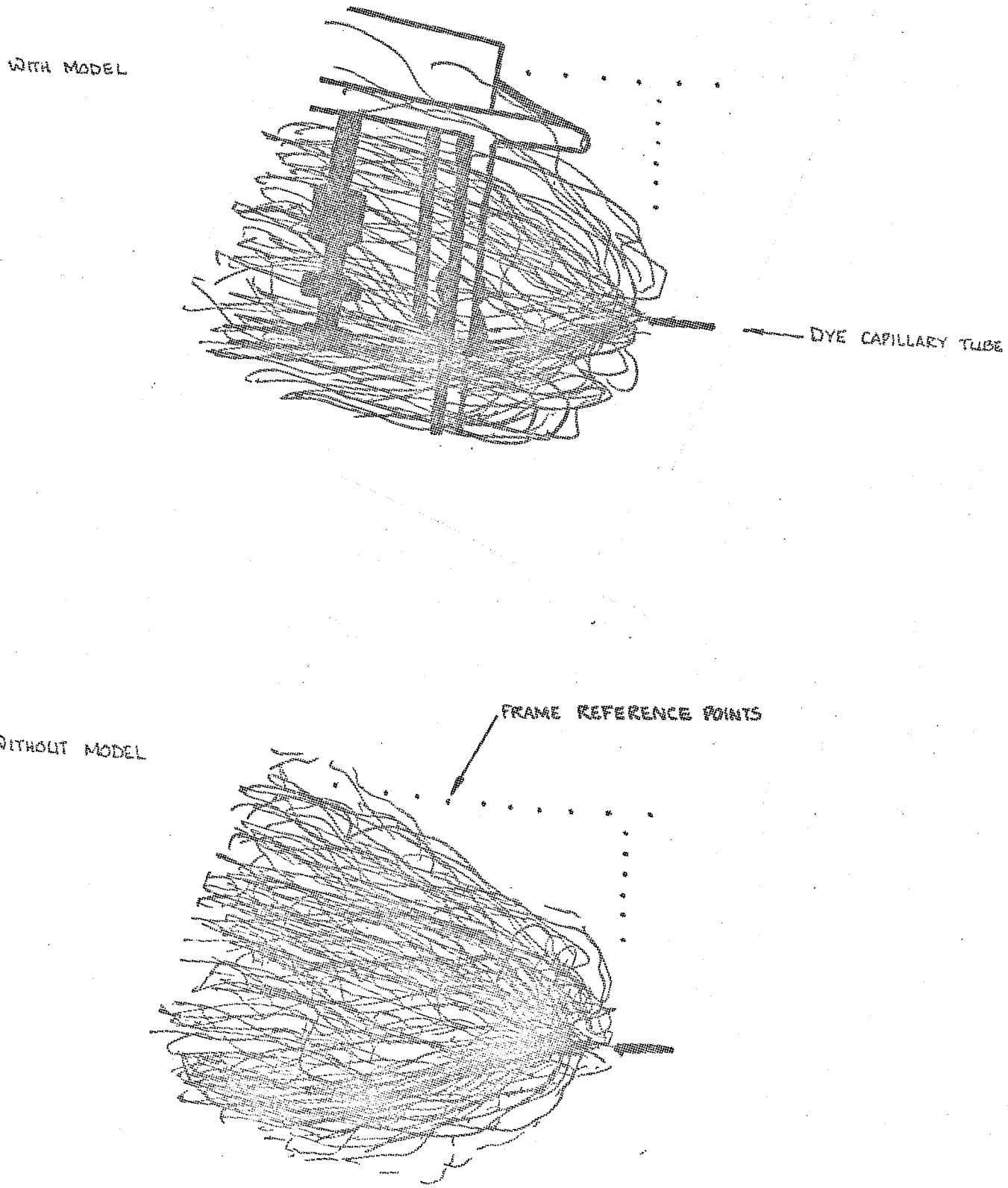

FIG. 10 MODEL ON GROUND-BOARD AT TOW SPEED OF 40 cm/s.

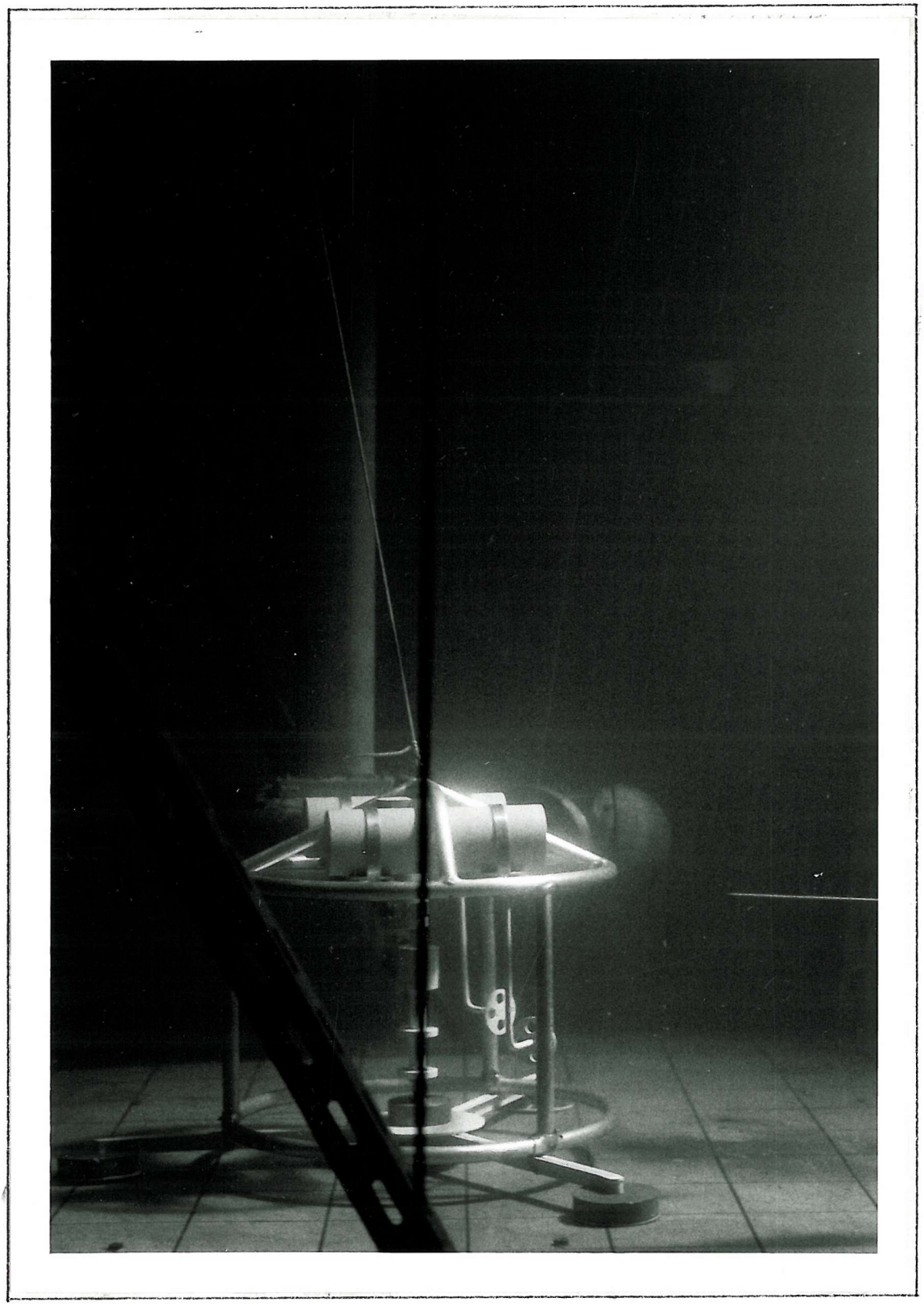

FIG. 11 BUOYANCY LIFT-DRAG MEASUREMENT.

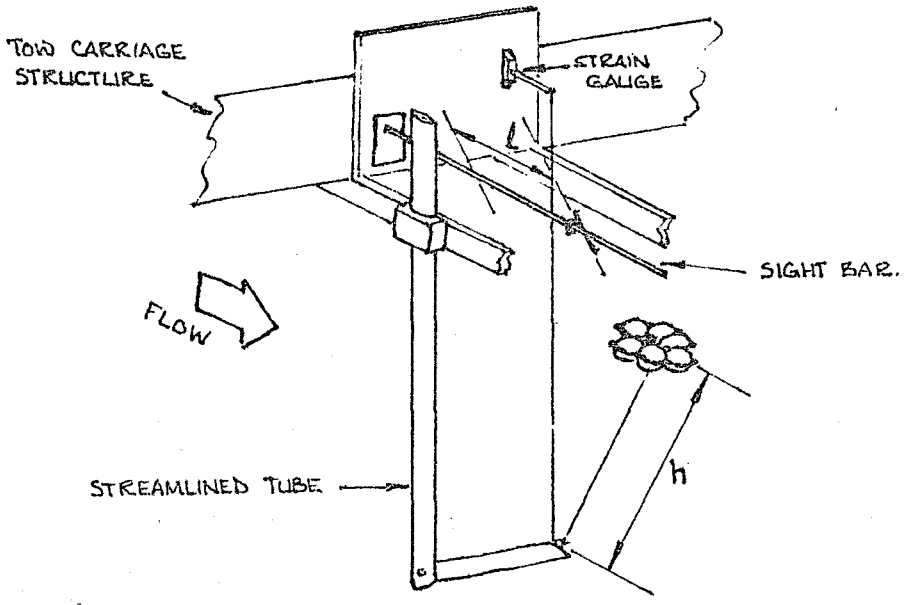

EXPERIMENT SET UP

BUOYANCY ARRANGEMENTS INVESTIGATED

"6 IN A RING"

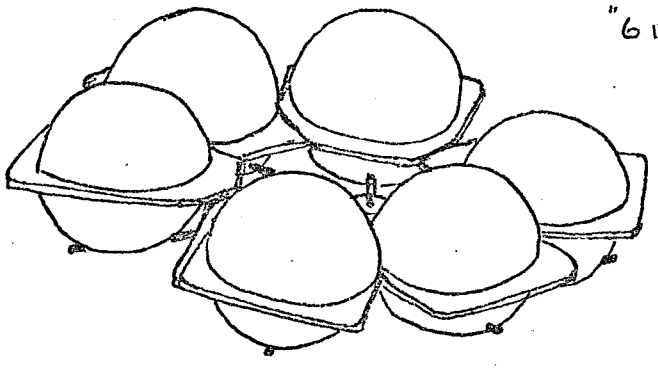

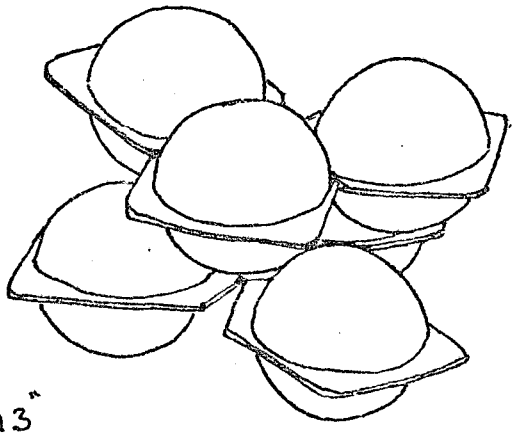

"3 ON 3"